

What, if anything, is the true neurophysiological significance of “rotational dynamics”?

Mikhail A. Lebedev^{1-3*}, Nil Adell Mill⁴, Núria Armengol Urpí⁵, Maria R. Cervera⁴, and Miguel A.L. Nicolelis^{1,6-10*}

¹Duke Center for Neuroengineering, Duke University, Durham, NC, USA; ²Center for Bioelectric Interfaces of the Institute for Cognitive Neuroscience of the National Research University Higher School of Economics, Moscow, Russia; ³Department of Information and Internet Technologies of Digital Health Institute, I.M. Sechenov First Moscow State Medical University, Moscow, Russia; ⁴Institute of Neuroinformatics, University of Zurich and ETH Zurich, Switzerland; ⁵D-MAVT ETH Zurich, Switzerland; ⁶Department of Neurobiology, Duke University Medical Center, Durham, NC, USA; ⁷Department of Neurology, Duke University, Durham, NC, USA; ⁸Department of Neurosurgery, Duke University, Durham, NC, USA; ⁹Department of Psychology and Neuroscience, Duke University, Durham, NC, USA; ¹⁰Edmond and Lily Safra International Institute of Neurosciences of Natal, Natal, Brazil

*Correspondence: mikhail.lebedev@gmail.com; nicoleli@neuro.duke.edu

Back in 2012, Churchland and his colleagues proposed that “rotational dynamics”, uncovered through linear transformations of multidimensional neuronal data, represents a fundamental type of neuronal population processing in a variety of organisms, from the isolated leech central nervous system to the primate motor cortex. Here, we evaluated this claim using Churchland’s own data and simple simulations of neuronal responses. We observed that rotational patterns occurred in neuronal populations when (1) there was a temporal shift in peak firing rates exhibited by individual neurons, and (2) the temporal sequence of peak rates remained consistent across different experimental conditions. Provided that such a temporal order of peak firing rates existed, rotational patterns could be easily obtained using a rather arbitrary computer simulation of neural activity; modeling of any realistic properties of motor cortical responses was not needed. Additionally, arbitrary traces, such as Lissajous curves, could be easily obtained from Churchland’s data with multiple linear regression. While these observations suggest that “rotational dynamics” depict an orderly activation of different neurons in a population, we express doubt about Churchland et al.’s exaggerated assessment that this activity pattern is related to “an unexpected yet surprisingly simple structure in the population response” which “explains many of the confusing features of individual neural responses.” Instead, we argue that their rotational dynamics approach provides little, if any, insight on the underlying neuronal mechanisms employed by neuronal ensembles to encode motor behaviors in any species.

Introduction

It is well known that individual neurons in cortical motor areas transiently modulate their firing rates following a stimulus that triggers the production of a voluntary movement (Evarts 1972). These neuronal modulations have been shown to represent various motor parameters, for example movement direction (Georgopoulos, Kalaska et al. 1982), although the specifics of these representations are still a matter of debate (Georgopoulos, Ashe et al. 1992, Kakei, Hoffman et al. 1999, Zhuang, Lebedev et al. 2014). With the development of multichannel recordings (Nicolelis, Dimitrov et al. 2003, Schwarz, Lebedev et al. 2014), it has become possible to study modulations recorded in multiple cortical neurons simultaneously. This methodological advance led to many studies attempting to uncover how neuronal populations process information (Chapin and Nicolelis 1999, Laubach, Shuler et al. 1999,

Averbeck and Lee 2004, Nicolelis and Lebedev 2009).

Among the studies on motor and premotor cortical neuronal populations, one paper by Churchland and his colleagues (Churchland, Cunningham et al. 2012) became especially popular. In their work, Churchland et al. claimed to have discovered a unique property of cortical population activity that they called “rotational dynamics.” Their analysis is based on the idea that motor cortical activity could be modeled as a dynamical system:

$$\dot{X} = M_{skew}X \quad (1)$$

where X is a multidimensional vector representing neuronal population activity, \dot{X} is its time derivative and M_{skew} is the transform matrix. M_{skew} has imaginary eigenvalues, which means that \dot{X} is orthogonal to X (Garfinkel,

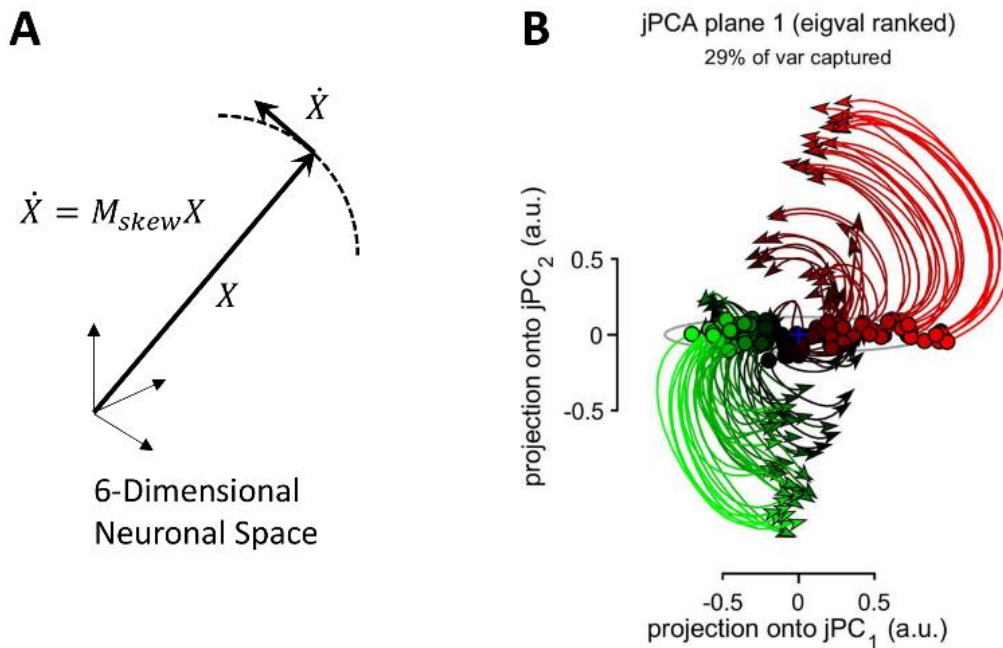


Figure 1. rotation in a multidimensional neuronal space. **A:** Schematics of “rotational dynamics”, where there is an angle between the neuronal vector, X , and its time derivative, \dot{X} , meaning that X is turning. In jPCA proposed by Churchland et al. (2012), X is formed by the first six PC of the population activity. **B:** Application of jPCA to neuronal data. Curves represent experimental conditions, where a monkey performed armed reaching with different trajectories. The color of the curves (red, green, black) corresponds to different levels of premovement activity.

Shevtsov et al. 2017), which corresponds to X rotating (Figure 1A). In the analysis of Churchland et al., vector X is produced from the activity of neuronal populations by the application of principal component analysis (PCA). The first six principal components (PCs) are selected to avoid overfitting that could take place with a larger number of dimensions. Hence, X is six-dimensional. Next, a method called jPCA is applied to compute M_{skew} and the corresponding eigenvectors. Churchland et al. projected PC data to the plane defined by the first two most prominent rotational components generated with jPCA and obtained convincing looking figures, where population responses rotated in the same direction for different experimental conditions (Figure 1B).

According to the interpretation of Churchland et al., “rotational dynamics” are a fundamental feature of population activity in the motor and premotor cortical areas and a proof that motor cortical populations act as a dynamical system rather than representing various motor parameters by their firing. They called the rotational effect an “orderly rotational structure, across conditions, at the population level”, a “brief but strong oscillatory component, something quite unexpected for a non-periodic behavior”, and “not trivial”

observations that are “largely expected for a neural dynamical system that generates rhythmic output.”

While this proposal has merits, we found the results of Churchland et al. difficult to comprehend because of the lack of clarity regarding the concrete neuronal patterns contributing to the rotations revealed by jPCA. For example, they suggested that “motor cortex responses reflect the evolution of a neural dynamical system, starting at an initial state set by preparatory activity [...]. If the rotations of the neural state [...] reflect straightforward dynamics, then similar rotations should be seen for all conditions. In particular, the neural state should rotate in the same direction for all conditions, even when reaches are in opposition” – a statement that is hard to understand without a clarification of concrete features of neuronal responses that contribute to rotations. For instance, it is unclear what “straightforward dynamics” are and why they impose the same rotational patterns on all conditions. The major obstacle to understanding the ideas expressed by Churchland and his colleagues is the absence of a clear explanation of how individual neurons and/or their populations contribute to the presumably oscillatory patterns revealed by jPCA.

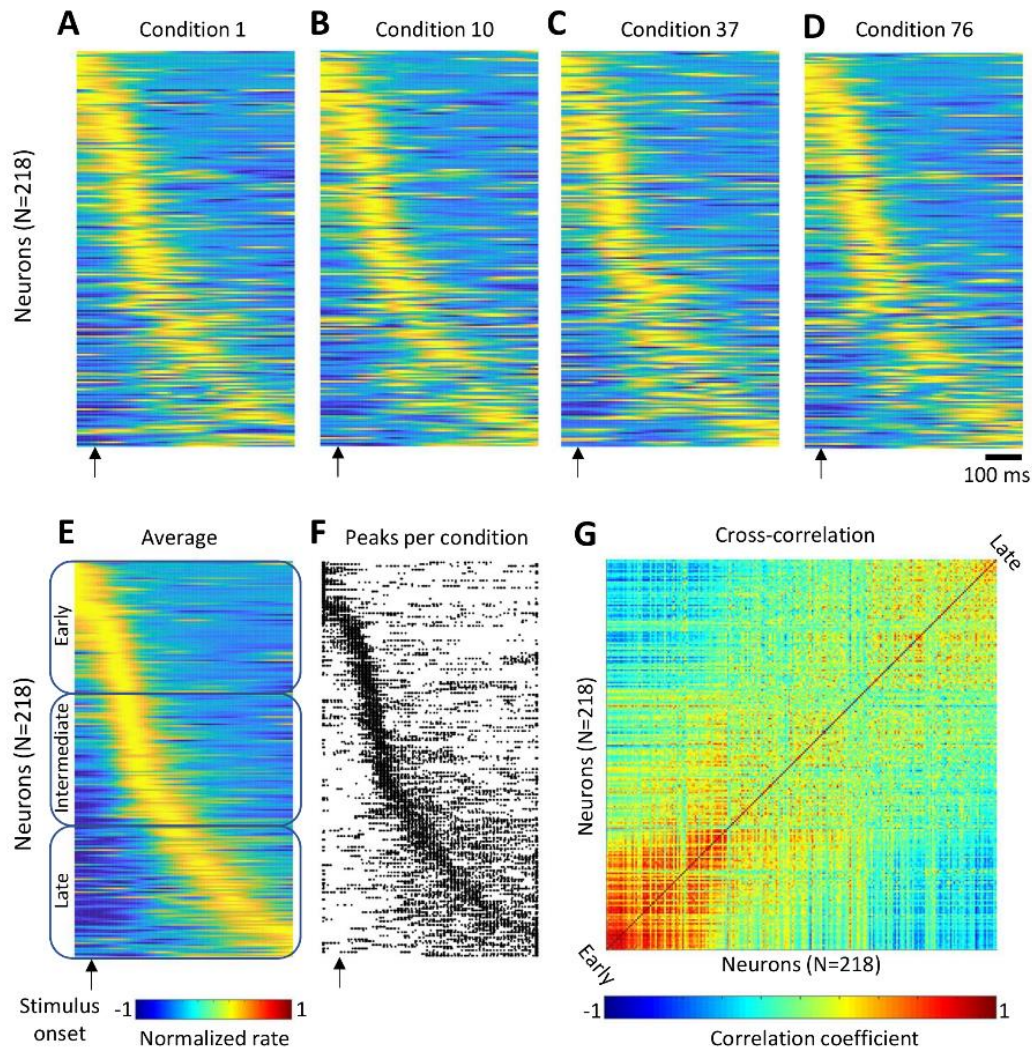


Figure 2. Time spread in peak firing rates of different neurons in the data provided by Churchland et al. (2012). **A-D:** Color-coded population PETHs for four representative conditions. Horizontal lines represent PETHs for individual neurons. **E:** PETHs averaged across conditions. From top to bottom: neurons are ordered by the time of peak firing rate, from the earliest activated neurons to the latest. The same order is used in A-D, F and G. The neuronal population was divided into three subpopulations: early (neurons 1-73), intermediate (74-146), and late (147-218). **F:** A scatterplot showing the times of peak firing rates for different neurons and conditions. Peak times are represented by dots. **G:** Pairwise correlation between the activity patterns of different neurons.

To eliminate this gap in understanding, we reanalyzed some of the data that Churchland et al. made available online. We utilized perievent time histograms (PETHs), a basic method for displaying neuronal data, to find the underlying cause for the “rotational dynamics.” Next, we ran simple simulations to verify our findings. Based on our results, we found the interpretation offered by Churchland et al. highly overstated and overreaching. Even though the “rotational dynamics” appear to represent a certain temporal order in which different cortical neurons are activated during a behavioral task, and which is consistent across conditions, we are not convinced that this observation could significantly “help transcend

the controversy over what single neurons in motor cortex code or represent,” as stated by Churchland and his colleagues.

Results

Rotation in a multidimensional neuronal space could be thought of as a process where individual neurons are activated in a certain order, which results in the neuronal vector X changing orientation (Figure 1A). Such a pattern can be also described as a phase shift between the responses of different neurons. Consider the simplest case of a population that consists of two neurons where the activity of the first neuron is a sine function of time and activity of the second neuron is a cosine. Since the phase

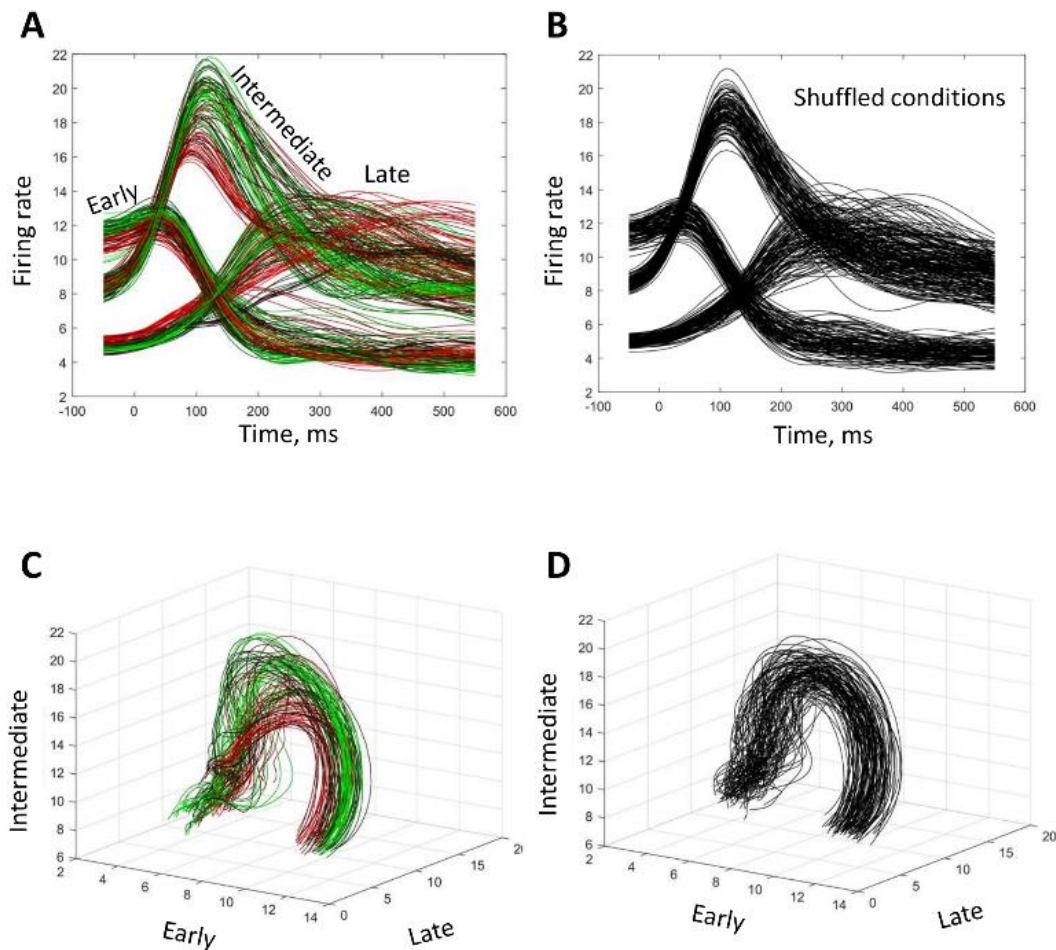


Figure 3. “Rotational dynamics” revealed by splitting neuronal population into the early, intermediate and late activated subpopulations. **A:** Average PETHs for the three subpopulations, for different experimental conditions. The composition of the subpopulations is shown in Figure 2E. Color coding of the traces is the same as in Figure 1B. **B:** Average PETHs for the shuffled-conditions data. **C,D:** “Rotational dynamics” shown as three-dimensional plots with the axes representing average PETHs for different subpopulations. Original (C) and shuffled (D) datasets are shown.

shift between the responses of these neurons is 90 degrees, a two-dimensional plot with the firing rates of these neurons on the axes produces circular or elliptical trajectories. This type of trajectory is observed for all conditions if the phase shift between the neurons persists.

Following this logic, we hypothesized that the data of Churchland et al. contained phase shifts between the neurons, which remained consistent across conditions. To test this hypothesis, we analyzed their data using the traditional PETH method. The dataset included PETHs of 218 neurons calculated for 108 experimental conditions (i.e., one smoothed PETH per condition; single-trial data were unavailable). Each condition corresponded to a monkey performing a reaching movement with a straight or convoluted trajectory. We simply stacked these PETHs to produce population color plots for different conditions (Figure 2A-D). Additionally, we averaged the PETHs across all

conditions to obtain average responses for each neuron (Figure 2E). For the average PETHs, we calculated peak values and reordered the neurons according to the value of the time when each neuron reached its peak firing rate. In the color plot showing the average PETHs (Figure 2E), PETHs of the neurons activated early are plotted at the top and PETHs of the neurons activated late are plotted at the bottom, which results in a clear display of an activity wave running across the neurons in the population. The same reordering was applied to the PETHs for individual conditions (Figure 2A-D). In the PETHs for individual conditions, the temporal order of responses persisted with some jitter (e.g., compare panels A, B, C and D in Figure 2). The same sequence of responses is also clear in the scatterplot that displays the time of peak response for different conditions and different neurons (Figure 2F). Additionally, pairwise correlations were strong for the neurons with

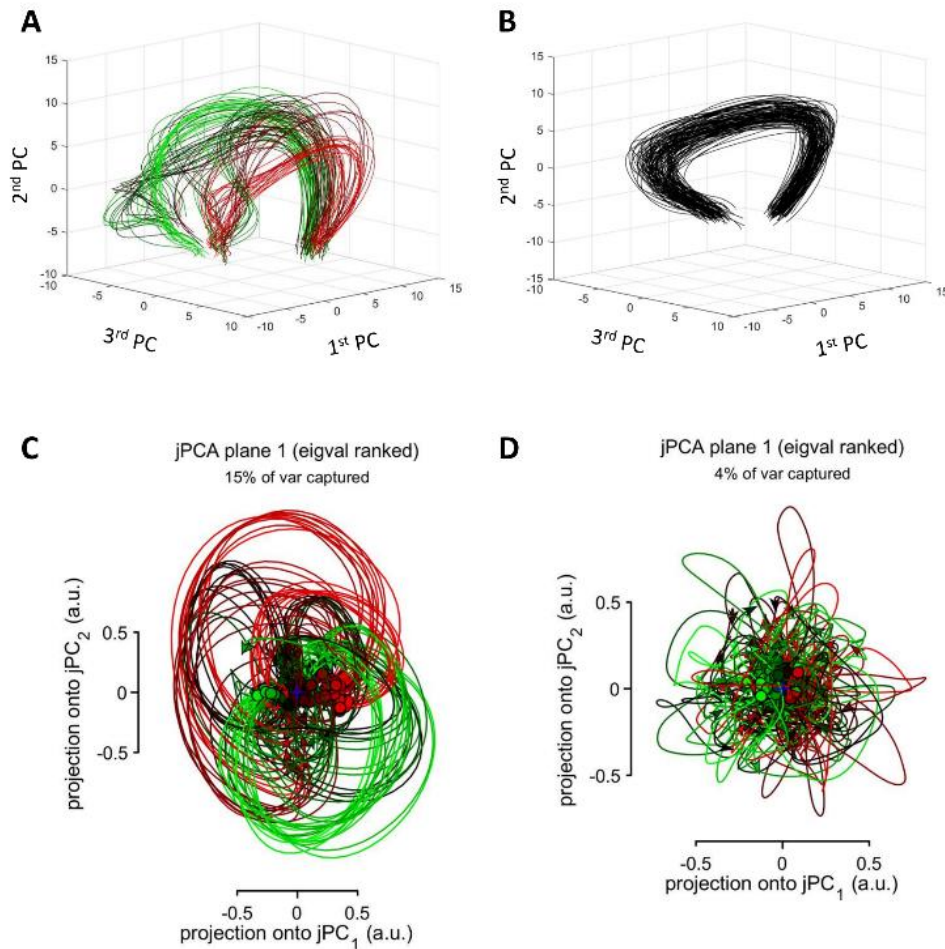


Figure 4. Rotations of principal components. **A:** The first three PCs plotted as a three-dimensional plot. Color conventions as in Figure 1B. **B:** PCs for the data with shuffled conditions. **C:** jPCA results for the data in A. **D:** jPCA results for the data in B.

similar occurrences of response and weak (or negative) for the neurons with dissimilar occurrences (Figure 2G). Thus, the PETH analysis showed that in Churchland's data neurons responded in a certain temporal order, and this order persisted even when the monkey altered the way it performed a reaching movement.

To assess how the activation order of different neurons could contribute to a population rotational pattern, we split the entire neuronal population into three subpopulations: neurons with early peaks (ranks 1-73), intermediate peaks (74-146), and late peaks (147-218) (Figure 2E). Next, we calculated average PETHs for each subpopulation and for each experimental condition (Figure 3A). As expected, this plot revealed three groups of PETHs (early-peak, intermediate-peak and late-peak) whose shapes did not change substantially across conditions. Plotting these PETHs in a three-dimensional space (where dimensions corresponded to the subpopulations) yielded a family of curved trace (Figure 3C) that

resembled the circles obtained with jPCA (Figure 1B). As an additional control, we randomly shuffled conditions for each neuron and plotted the curves for the shuffled data (Figure 3B,D). Both the average PETHs for the subpopulations (Figure 3B) and the three-dimensional plot (Figure 3D) were little affected by the shuffling procedure, which confirmed that the activation order of the neurons was approximately the same for different conditions.

To further clarify the origin of the rotational patterns, we calculated the initial three PCs for the data of Churchland et al. and plotted them as a three-dimensional plot (Figure 4A). The PC traces were clearly curved. Additionally, distinct clusters of conditions were visible in the plots, each of them containing several traces that had similar shapes. The clusters started from approximately the same point but separated toward the end of the trial. Despite the differences between the clusters, they rotated in approximately the same fashion (e.g., in the plane defined by the first and second PCs). Thus,

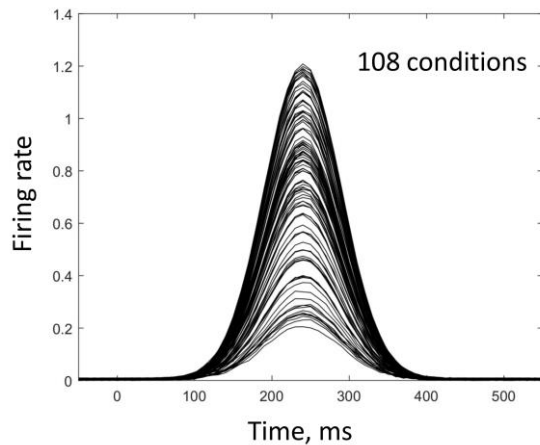


Figure 5. Simulated responses for an individual neuron. Neuronal responses were simulated using a Gaussian function. Response amplitude was randomly drawn from a uniform distribution (in the interval 0.2-1.2).

“rotational dynamics” were clearly visible even before the application of jPCA. As to JPCA, it also yielded several clusters of circles (Figure 4C). Rotations continued to be present after experimental conditions were randomly shuffled for each neuron, which indicated that condition-specific correlation between the responses of different neurons was not crucial for a rotational pattern to occur. Indeed, the PC traces for the shuffled data were clearly curved, although the clusters of curves were removed by the shuffling procedure (Figure 4B). Curiously, jPCA failed to detect this curvature and returned noisy traces (Figure 4D), apparently because the algorithm operated on the ill-conditioned data (Golub and Van Loan 2012) produced from very similar entries for different conditions. (jPCA encounters the same problem, for example, for a simple simulation where responses of a half of the neurons are a sine function of time and responses of the other half are a cosine. Although this is an obvious case of “rotational dynamics,” because of the data being ill-conditioned, the jPCA algorithm fails to produce circles. This problem can be handled by shifting the responses of simulated neurons in time for different conditions; see below.)

Having established that neurons were activated in consistent temporal order in Churchland’s data, we examined this effect further using a simulation of population activity. The simulation was very simple and did not incorporate any specific features of motor cortical responses. For example, simulated neurons were not directionally tuned and instead each of them exhibited random amplitude of response for different conditions.

Because of this randomness, response amplitude was not correlated in any pair of neurons. The only nonrandom pattern that we simulated was the presence of a sequence of responses in different neurons. The shape of simulated PETHs was a Gaussian function with an amplitude drawn from a uniform distribution (Figure 5). We simulated 218 neurons and 108 conditions to match Churchland’s data.

Recently, Michaels, Dann et al. (2016) used a somewhat similar simulation of neurons having a temporal sequence of responses, and observed an occurrence of “rotational dynamics” under these conditions. Their simulation was more sophisticated than ours as they attempted to simulate realistic properties of motor cortical neurons, such as cosine-shaped directional tuning. To prove that jPCA reveals some important properties of motor cortical activity, they performed data permutations of different complexity. Yet, they did not consider the possibility that some of these permutations could make data ill conditioned for jPCA. In our simulation, resemblance to motor cortical activity was minimal. We also applied a simple correction to cope with the ill conditioned data.

We started with a simulation, where the responses of different neurons were shifted in time: neuron i responded 10 ms later than neuron $i-1$ (Figure 6A). This simulation produced a wave of activity running through the neuronal population. Since the population responses were very similar for different conditions, the data was ill-conditioned, and jPCA analysis returned noise (Figure 6B) even though the input data contained the major ingredient of “rotational dynamics.” This problem of ill-conditioning could be easily solved by introducing some variability to the conditions. We simulated two groups of conditions: for conditions 1-54, the first neuron exhibited peak activity at time $t = 50$ ms, and for conditions 55-108 the time of its peak activity was $t = 200$ ms (Figure 6C). The structure of the activity wave (i.e. the rule that neuron i responded 10 ms later than neuron $i-1$) was the same for both groups of trials. Such groups of trials would occur if a monkey on some trials waited for an additional 150 ms before initiating the movement. This slight alteration of the data, which did not change the structure of the population response at all, was sufficient for jPCA to start generating circles (Figure 6D). We also simulated three groups of conditions, where the first neuron’s peak rate occurred at 50, 150 and 200 ms for the first, second and third groups, respectively

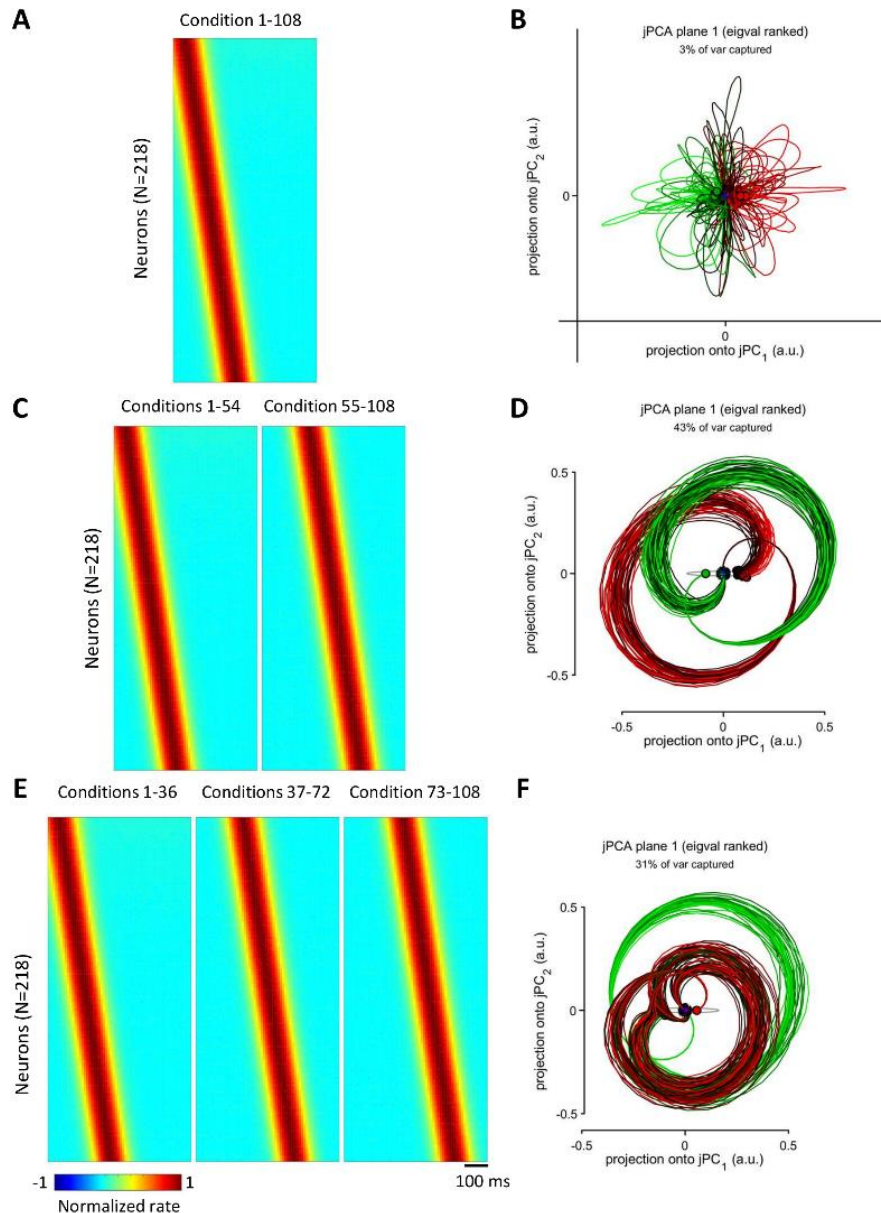


Figure 6. Simulated population responses with a time spread of peak firing rates. **A:** PETHs for a simulated wave of population activity, where response of neuron i occurs 10 ms later than response of neuron $i-1$. **B:** jPCA results for the data in A. **C:** The same population wave as in A with an early onset for conditions 1-54 and late onset for conditions 55-108. **D:** jPCA results for the data in C. **E:** The same population wave as in A and C with three different onsets for conditions 1-36, 37-72 and 73-108. **F:** jPCA results for the data in E.

(Figure 6E). The structure of the population wave was the same for all three groups. In this case, again, jPCA returned circles (Figure 6F).

To verify that a temporal sequence of activation was necessary for the rotation pattern to occur, we simulated neuronal populations without any spread in peak activity times (Figure 7). The shapes of neuronal responses were the same as in the previous simulation (Figure 5). In this case, jPCA failed to generate circles (Figure 7B) even when three groups of conditions were simulated with shifted activity onsets (Figure 7A).

Finally, we probed a more direct approach for converting Churchland’s data into circular trajectories. Churchland et al. linearly fit the population activity vector to its first derivative (equation 1) with the goal of extracting a rotational structure. We assumed that such an extraction of a desired “population property” could be achieved with a multiple linear regression. Accordingly, we utilized multiple linear regression to fit neuronal data to a circle:

$$x = \cos \frac{2\pi t}{T}; y = \sin \frac{2\pi t}{T} \quad (2)$$

or to the Lissajous curve shaped as ∞ :

$$x = \cos \frac{2\pi t}{T}; y = \sin \frac{4\pi t}{T} \quad (3)$$

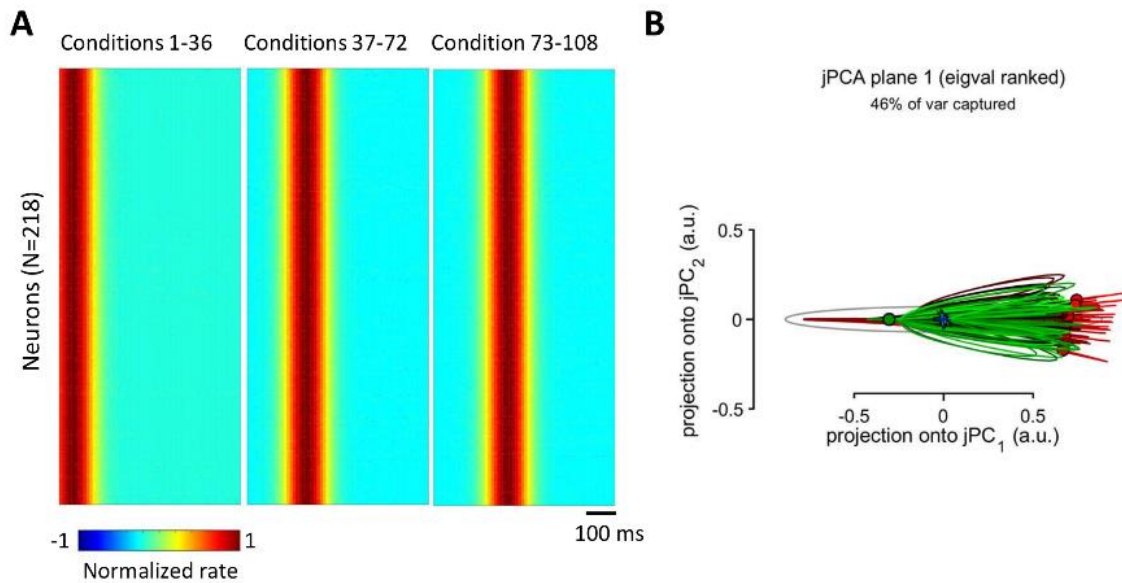


Figure 7. Simulated population responses without a time spread of peak firing rates. A: PETHs with different response onsets for conditions 1-36, 37-72 and 73-108. For each group of conditions, peak responses of different neurons were not spread in time. **B:** jPCA results for the data in A.

where t is time and T is trial duration. The regression worked well for both shapes (Figure 8A,B), and it even generalized to new conditions, as evident from the analysis where half of the data were used for training the regression model and the other half for generating predictions (Figure 8C,D). The shuffled data could be fit to the Lissajous curves, as well (Figure 8E-H), although the prediction of ∞ was very noisy (Figure 8H).

Discussion

To clarify the neurophysiological significance of “rotational dynamics,” we conducted additional analyses of Churchland’s data and performed simple simulations. In the original dataset, we discovered a temporal order in which the neurons were activated and found that this order was relatively consistent across conditions. In our opinion, this is a useful observation that has not been described in sufficient detail in the original article of Churchland et al. and the publications that emerged from this study. We suggest that simple plots of population PETHs (e.g., Figure 2) could be helpful to clarify jPCA results and demystify “rotational dynamics.” For example, plotting PETHs for the neuronal population being considered could add substance to claims like the “rotational dynamics” persist even though motor-related patterns are different across condition (Churchland, Cunningham et al. 2012) or the recurrent neural network trained to

generate arm-muscle EMGs develops rotational patterns (Sussillo, Churchland et al. 2015).

The existence of a temporal spread in neuronal peak rates (or response latencies) has been documented in the literature. For example, waves of activity similar to those shown in Figure 2E-F have been depicted in many previous publications (Luczak, Barthó et al. 2007, Gage, Stoetzner et al. 2010, Peyrache, Benchenane et al. 2010, Kvitsiani, Ranade et al. 2013, Bulkin, Law et al. 2016). Regarding motor cortical patterns during reaching, Figure 7 in Georgopoulos et al. (Georgopoulos, Kalaska et al. 1982) shows a distribution of the times of onset of the first increase in discharge in motor cortical neurons for center-out arm reaching movements performed by a monkey. The onsets were calculated for the neurons’ preferred directions and ranged -300 to 500 ms relative to movement initiation time. In a more recent paper (Ifft, Lebedev et al. 2011), we have demonstrated such a spread for simultaneously recorded populations of neurons recorded in the motor and primary somatosensory cortical areas.

It may be true that no previous paper focused on the consistency of neuronal activation order for a range of movements. Yet, Churchland and his colleagues did not emphasize such consistency either and instead emphasized variability of neuronal responses across conditions. According to their explanation, rotational patterns are principally a population phenomenon that persists despite

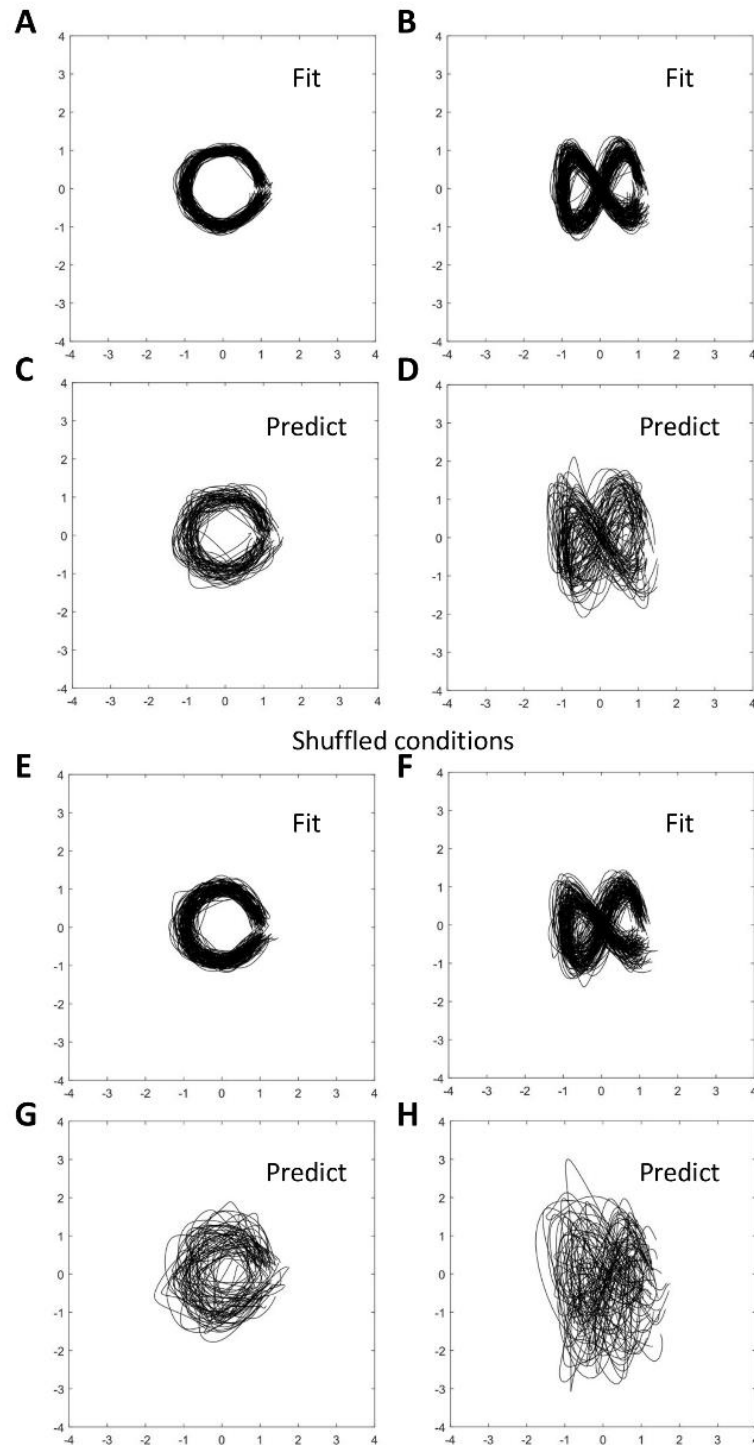


Figure 8. Fitting population data to Lissajous curves. A: Fitting to a circle. B: Fitting to the curve shaped as ∞ . C: Prediction of a circle. Half of the conditions were used to train the regression model; the other half to generate prediction. D: Prediction of the ∞ shape. E-H: Fitting and predicting for the data with shuffled conditions.

individual neurons exhibiting different activity patterns for different arm reaches.

Temporal sequences of neuronal responses that are consistency across a set of experimental conditions could occur for various reasons. For example, such a temporal order could be related to serial information processing by a neuronal

circuit. Orderly response onsets have been reported for the activity of multiple cortical areas transforming sensory inputs into behavioral actions. For example, de Lafuente and Romo (2006) reported that a wave of neuronal activity travelled from the somatosensory cortex to the premotor cortical

areas when monkeys performed a task that required perceptual judgment of a tactile stimulus. Sensorimotor transformation of this kind could be analyzed using a comparison of response characteristics for different cortical locations and different types of neurons. Unfortunately, jPCA makes such an analysis impossible because it lumps the activity of many neurons together (e.g. compare Figure 2 with Figure 4C).

Based on our observations, we question that Churchland's results provide a strong evidence in favor of the dynamical-system model of motor cortical processing as opposed to representational models, where neuronal populations process concrete motor variables and goals, such as movement direction. This is because the presence of a sequence of neuronal responses is not something unique for a dynamical system that acts "like a spring box" that "could be released to act as an engine of movement" (a quote from Michaels, Dann et al. (2016)). For instance, the mere fact that one neuron responds before the other one does not prove that these neurons are parts of the same dynamical system; there could be no meaningful interconnection between them. Thus, jPCA would generate rotations even for a population composed from the neurons recorded in different monkeys performing reaching movements.

It is obvious that sequences of responses (and associated jPCA-generated rotations) could be observed in many parts of the nervous system. For example, in a sensory system, peripheral afferents respond to the stimulus first, followed by neuronal responses in the spinal cord, brainstem nuclei, thalamus and eventually the cortex. Although this processing chain could be called a dynamical system, this definition alone does not clarify any issue of sensory processing. As far as motor systems are concerned, they are known to perform sensorimotor transformations (Georgopoulos, Lurito et al. 1989, Kalaska 1991), where some neurons are more representative of the sensory inputs, such as go-cues, and the other handle the later occurring events, such as motor execution and even reward representation. Saying that "rotational dynamics" occurs during this sensorimotor transformation only adds terminology but does not solve any concrete issue related neuronal mechanisms of motor control.

According to Churchland et al., "a focus on the dynamics that generate movement will help transcend the controversy over what single

neurons in motor cortex code or represent." While we agree with this general idea, their jPCA result do not appear to advance our understanding of cortical mechanisms of motor control. Rotations demonstrated with jPCA are not something specific to motor cortical processing. Such patterns could be obtained with little effort using simple and quite arbitrary simulations that did not mimic any important property of motor cortical activity, such as directional tuning. It was sufficient for the simulated neurons to respond in a certain temporal sequence for "rotational dynamics" to occur. This observation suggests that the existence of rotation tells us very little about the function of motor cortical areas. Instead, jPCA appears to be just a way to illustrate the presence of phase shifts between the responses of different neurons rather than a method that provides insights to the underlying neurophysiological mechanisms ruling the function of the motor cortex.

While jPCA appears to detect the presence of a consistent temporal sequence of neuronal responses in certain case, we are not convinced that this analysis performs well in all cases. For example, we observed that the sequence of responses persisted following data shuffling across conditions (Figure 3B,D; Figure 4B) but jPCA failed to detect this sequence because the data became ill conditioned for this particular analysis (Figure 4D). Simple PETHs (Figure 2A-E) and regular PCA (Figure 4A,B) may be more reliable methods than jPCA for detecting response sequences and curved phase trajectories.

Mathematically, Churchland's method to produce a rotating pattern from neuronal PETHs can be described as a linear transformation with a certain number of free parameters. With a sufficient number of free parameters, multiple linear regression can yield practically any desired curve (Babyak 2004). For example, when we applied a multiple linear regression to Churchland's data, we easily produced a variety of Lissajous curves. Because of the similarity of neuronal responses across conditions, this transformation even generalized from the training dataset (half of the conditions) to new data in the test dataset (the other half) (Figure 8). Evidently, no one would claim that any of these arbitrarily chosen curves represents a physiologically meaningful neural population mechanism, although we used a linear transformation very similar to the one Churchland and his colleagues employed to generate their curves.

Altogether, our results challenge the conclusions of Churchland and his colleagues. Clearly, their effects simply reflect what one should expect by applying a linear transformation, such as PCA, to reduce the dimensionality of large-dimension data and then adjusting the resulting components to a new basis that reproduces a desired behavior (in this case rotation). PCA (Chapin and Nicolelis 1999) and independent component analysis (Laubach, Shuler et al. 1999) were introduced twenty years ago by our group to extract correlated neuronal patterns and reduce dimensionality of neuronal-ensemble data. While the findings of Churchland and his colleagues can be viewed as an extension of this approach and a method to produce a visually appealing phase plot, we doubt that they have discovered any new neurophysiological mechanism, as claimed in their article. Indeed, the mere fact that neurons in a population respond at different times with respect to a go-cue tells very little about the function of these responses and does not discard any of the previously proposed representational interpretations, such as the suggestion that neuronal populations perform a sensorimotor transformation (Georgopoulos, Lurito et al. 1989, Kalaska 1991, Kakei, Hoffman et al. 2003) or handle specific motor parameters (Georgopoulos, Kalaska et al. 1982, Georgopoulos, Ashe et al. 1992, Kakei, Hoffman et al. 1999, Zhuang, Lebedev et al. 2014).

Cortical activity is dynamical in the sense that neuronal rates change in time. Differential equations (Lukashin and Georgopoulos 1993) and other mathematical methods (Kawato and Wolpert 1998, Moody and Zipser 1998, Todorov 2000) are certainly applicable to modeling these dynamics. However, a much more thorough analysis compared to the method proposed by Churchland et al. is needed for making a major advance in our understanding of cortical mechanisms of motor control.

Methods

The data (single units and good multiunits recorded in monkey N; the data used to construct Fig. 3f of Churchland et al.) and MATLAB scripts were obtained from Churchland lab's online depository (<https://www.dropbox.com/sh/2q3m5fqfscwf95j/AAC3WV90hHdBgz0Np4RAKJpYa?dl=0>). The dataset contained PETHs for each neuron and each condition. We used the following commands to run Churchland's code:

```
times = -50:10:550; (4)
jPCA_params.numPCs = 6;
```

```
[Projection,Summary]=jPCA(Data,times,jPCA_params);
```

This corresponds to the time range -50 to 550ms and six PCs entered in jPCA.

To produce the plots shown in Figure 2A-D, we stacked Churchland's PETHs together, and Figure 2E shows PETHs averaged across conditions. The average PETHs were used to find peak firing rates and the time of their occurrences. PETHs of Figure 2A-E were sorted according to the sequence of these peaks of the average PETHs. To improve the display of phase shifts between the neurons, PETHs of Figure 2A-E were normalized by subtracting the mean and dividing by the peak PETH value. This normalization was used only for plotting the graphs of Figure 2A-E but not for calculating average PETHs for individual neurons (Figure 2E) or neuronal subpopulations (Figure 3).

In the PCA analysis (Figure 4), we standardized PETHs for each neuron by subtracting the overall mean (i.e., average for all conditions combined) and dividing by the overall standard deviation (again, for all conditions combined).

Simulated PETHs (Figure 5) were computed in MATLAB as:

$$PETH = \exp(-(times-tau).^2/50)*(0.2+rand(1)); \quad (5)$$

where the time shift, τ , was selected to produce 10-ms increments of the delay for the neurons in the sequence (Figure 6). Neither the width of the response nor the amplitude (uniformly distributed from 0.2 to 1.2 in equation 5) were critical for the rotations to occur. However, to cope with the ill-conditioning of the population responses highly correlated across conditions, it was important to introduce temporal variability to the simulated PETHs. This was done by offsetting τ for all neurons by the same amount of time for several groups of conditions (Figure 6C,D).

Multiple linear regressions (Figure 8) were implemented in MATLAB (*regress* function). Here, neuronal activity was transformed into Lissajous curves. Fitting (Figure 8A,B,E,F) was conducted by using the same conditions as the training and test data. Predictions (Figure 8C,D,G,H) were computed by using half of the trials to train the regression model and the other half to test.

References

- Averbeck, B. B. and D. Lee (2004). "Coding and transmission of information by neural ensembles." *Trends in neurosciences* **27**(4): 225-230.
- Babjak, M. A. (2004). "What you see may not be what you get: a brief, nontechnical introduction to overfitting in regression-type models." *Psychosom Med* **66**(3): 411-421.

- Bulkin, D. A., L. M. Law and D. M. Smith (2016). "Placing memories in context: Hippocampal representations promote retrieval of appropriate memories." *Hippocampus* **26**(7): 958-971.
- Chapin, J. K. and M. A. Nicolelis (1999). "Principal component analysis of neuronal ensemble activity reveals multidimensional somatosensory representations." *Journal of neuroscience methods* **94**(1): 121-140.
- Churchland, M. M., J. P. Cunningham, M. T. Kaufman, J. D. Foster, P. Nuyujukian, S. I. Ryu and K. V. Shenoy (2012). "Neural population dynamics during reaching." *Nature* **487**(7405): 51-56.
- de Lafuente, V. and R. Romo (2006). "Neural correlate of subjective sensory experience gradually builds up across cortical areas." *Proceedings of the National Academy of Sciences* **103**(39): 14266-14271.
- Evarts, E. V. (1972). "Activity of motor cortex neurons in association with learned movement." *Int J Neurosci* **3**(3): 113-124.
- Gage, G. J., C. R. Stoetznner, A. B. Wiltschko and J. D. Berke (2010). "Selective activation of striatal fast-spiking interneurons during choice execution." *Neuron* **67**(3): 466-479.
- Garfinkel, A., J. Shevtsov and Y. Guo (2017). *Modeling life: the mathematics of biological systems*, Springer.
- Georgopoulos, A. P., J. Ashe, N. Smyrnis and M. Taira (1992). "The motor cortex and the coding of force." *Science* **256**(5064): 1692-1695.
- Georgopoulos, A. P., J. F. Kalaska, R. Caminiti and J. T. Massey (1982). "On the relations between the direction of two-dimensional arm movements and cell discharge in primate motor cortex." *J Neurosci* **2**(11): 1527-1537.
- Georgopoulos, A. P., J. T. Lurito, M. Petrides, A. B. Schwartz and J. T. Massey (1989). "Mental rotation of the neuronal population vector." *Science* **243**(4888): 234-236.
- Golub, G. H. and C. F. Van Loan (2012). *Matrix computations*, JHU press.
- Ifft, P., M. Lebedev and M. A. Nicolelis (2011). "Cortical correlates of Fitts' law." *Frontiers in integrative neuroscience* **5**: 85.
- Kakei, S., D. S. Hoffman and P. L. Strick (1999). "Muscle and movement representations in the primary motor cortex." *Science* **285**(5436): 2136-2139.
- Kakei, S., D. S. Hoffman and P. L. Strick (2003). "Sensorimotor transformations in cortical motor areas." *Neuroscience research* **46**(1): 1-10.
- Kalaska, J. (1991). *Reaching movements to visual targets: Neuronal representations of sensori-motor transformations*. Seminars in Neuroscience, Elsevier.
- Kawato, M. and D. Wolpert (1998). "Internal models for motor control." *Sensory guidance of movement* **218**: 291-307.
- Kvitsiani, D., S. Ranade, B. Hangya, H. Taniguchi, J. Huang and A. Kepecs (2013). "Distinct behavioural and network correlates of two interneuron types in prefrontal cortex." *Nature* **498**(7454): 363.
- Laubach, M., M. Shuler and M. A. Nicolelis (1999). "Independent component analyses for quantifying neuronal ensemble interactions." *Journal of neuroscience methods* **94**(1): 141-154.
- Luczak, A., P. Barthó, S. L. Marguet, G. Buzsáki and K. D. Harris (2007). "Sequential structure of neocortical spontaneous activity in vivo." *Proceedings of the National Academy of Sciences* **104**(1): 347-352.
- Lukashin, A. V. and A. P. Georgopoulos (1993). "A dynamical neural network model for motor cortical activity during movement: population coding of movement trajectories." *Biological cybernetics* **69**(5-6): 517-524.
- Michaels, J. A., B. Dann and H. Scherberger (2016). "Neural population dynamics during reaching are better explained by a dynamical system than representational tuning." *PLoS computational biology* **12**(11): e1005175.
- Moody, S. L. and D. Zipser (1998). "A model of reaching dynamics in primary motor cortex." *Journal of Cognitive Neuroscience* **10**(1): 35-45.
- Nicolelis, M. A., D. Dimitrov, J. M. Carmena, R. Crist, G. Lehew, J. D. Kralik and S. P. Wise (2003). "Chronic, multisite, multielectrode recordings in macaque monkeys." *Proceedings of the National Academy of Sciences* **100**(19): 11041-11046.
- Nicolelis, M. A. and M. A. Lebedev (2009). "Principles of neural ensemble physiology underlying the operation of brain-machine interfaces." *Nature reviews neuroscience* **10**(7): 530.
- Peyrache, A., K. Benchenane, M. Khamassi, S. Wiener and F. Battaglia (2010). "Sequential reinstatement of neocortical activity during slow oscillations depends on cells' global activity." *Frontiers in Systems Neuroscience* **3**(18).
- Schwarz, D. A., M. A. Lebedev, T. L. Hanson, D. F. Dimitrov, G. Lehew, J. Meloy, S. Rajangam, V. Subramanian, P. J. Ifft and Z. Li (2014). "Chronic, wireless recordings of large-scale brain activity in freely moving rhesus monkeys." *Nature methods* **11**(6): 670.
- Sussillo, D., M. M. Churchland, M. T. Kaufman and K. V. Shenoy (2015). "A neural network that finds a naturalistic solution for the production of muscle activity." *Nature neuroscience* **18**(7): 1025.
- Todorov, E. (2000). "Direct cortical control of muscle activation in voluntary arm movements: a model." *Nature neuroscience* **3**(4): 391.
- Zhuang, K. Z., M. A. Lebedev and M. A. Nicolelis (2014). "Joint cross-correlation analysis reveals complex, time-dependent functional relationship between cortical neurons and arm electromyograms." *J Neurophysiol* **112**(11): 2865-2887.